

Electric polarization induced by Néel order without magnetic superlattice: experimental study in $\text{Cu}_3\text{Mo}_2\text{O}_9$ and numerical one in a small spin cluster

Haruhiko KUROE^{1*}, Tomohiro HOSAKA¹, Suguru HACHIUMA¹, Tomoyuki SEKINE¹, Masashi HASE², Kunihiko OKA³, Toshimitsu ITO³, Hiroshi EISAKI³, Masashi FUJISAWA^{4†}, Susumu OKUBO⁴ and Hitoshi OHTA⁴

¹*Department of Physics, Sophia University, 7-1 Kioi-cho, Chiyoda-ku, Tokyo 102-8554, Japan*

²*National Institute for Materials Science (NIMS), Tsukuba, Ibaraki 305-0047, Japan*

³*National Institute of Advanced Industrial Science and Technology (AIST), Tsukuba, Ibaraki 305-8568, Japan*

⁴*Molecular Photoscience Research Center, Kobe University, 1-1 Rokko, 657-8501 Kobe, Japan*

We clarify that the antiferromagnetic order in the distorted tetrahedral quasi-one dimensional spin system induces electric polarizations. In this system, the effects of the low dimensionality and the magnetic frustration are expected to appear simultaneously. We obtain the magnetic-field-temperature phase diagram in $\text{Cu}_3\text{Mo}_2\text{O}_9$ by studying the dielectric constant and the spontaneous electric polarization. Around the tricritical point at 10 T and 8 K, the change of the direction in the electric polarization causes a colossal magnetocapacitance. We calculate the charge redistribution in the small spin cluster consisting of two magnetic tetrahedra to demonstrate the electric polarization induced by the antiferromagnetism.

KEYWORDS: multiferroic materials, frustrating magnet, charge redistribution, Mott insulator, distorted tetrahedral spin system

After the discovery of the strong magnetoelectric effect in TbMnO_3 ,¹⁾ multiferroics in transition metal oxides has been extensively studied.²⁾ In cases of the inverse Dzyaloshinskii-Moriya interaction in the spiral spin structure³⁻⁵⁾ and the inverse Kanamori-Goodenough interaction in the collinear one,⁶⁾ the formation of the magnetic superlattice plays an essential role in the magnetic-order induced multiferroics. The geometrical magnetic frustration also plays an important role as an origin of nontrivial spin configuration which breaks the spatial inversion symmetry. In this letter, we demonstrate that the distorted tetrahedral spin system has a potential to show the multiferroic behavior *without* any magnetic superlattice formation. We focus on the dielectric properties induced by an antiferromagnetic (AFM) spin order in $\text{Cu}_3\text{Mo}_2\text{O}_9$ and we discuss a possibility of the multiferroic behavior in AFM spin system, based on theory of the charge redistribution in frustrated Mott insulators.^{7,8)}

$\text{Cu}_3\text{Mo}_2\text{O}_9$ has two distorted tetrahedral quasi-one dimensional quantum spin systems of $S = 1/2$ spins along the b axis in its orthorhombic unit cell [Figs. 1(a) and 1(b)]. This compound

*E-mail address: kuroe@sophia.ac.jp

†Present address: Research Center for Low Temperature Physics, Tokyo Institute of Technology, Tokyo

has the geometrical magnetic frustrations due to the tetrahedral spin alignment and the quasi one-dimensionality simultaneously. This compound undergoes a AFM phase transition at $T_N = 7.9$ K without a magnetic field.^{9,10} The inelastic neutron scattering measurements clarify the hybridization effects due to the J_1 and J_2 superexchange interactions between two elemental magnetic excitations, i.e., that of the quasi one-dimensional AFM spin system made from the J_4 ($= 4.0$ meV) superexchange interactions and that of the isolated AFM spin dimers made from the J_3 ($= 5.8$ meV) ones.^{11,12}

The AFM spin-wave branch rises linearly from zero energy at the magnetic zone center of $(h, k, l) = (0, 1, 1)$, which is also the nuclear zone center below and above T_N . This magnetic branch is strongly dispersive along the $(0, k, 0)$ direction. This dispersion curve and the two-spinon continuum above a mass gap energy $\Delta = 1.2$ meV are typical features of a quasi-one dimensional AFM spin system. There are no indications of the formation of the commensurate or incommensurate magnetic superstructures, at least in our experimental resolution.

To obtain the magnetic-field-temperature (H - T) phase diagram, we measured the T and H dependences of the dielectric constant ϵ_α and the electric polarization P_α under an electric field E_α along the α axis ($\alpha = a$ or c) of $\text{Cu}_3\text{Mo}_2\text{O}_9$. In this letter, we focus on the effects of the magnetic field along the c axis. We prepared the plate-like single crystal of $\text{Cu}_3\text{Mo}_2\text{O}_9$ of which cross section and the thickness are typically about 60 mm^2 and 0.4 mm, respectively.

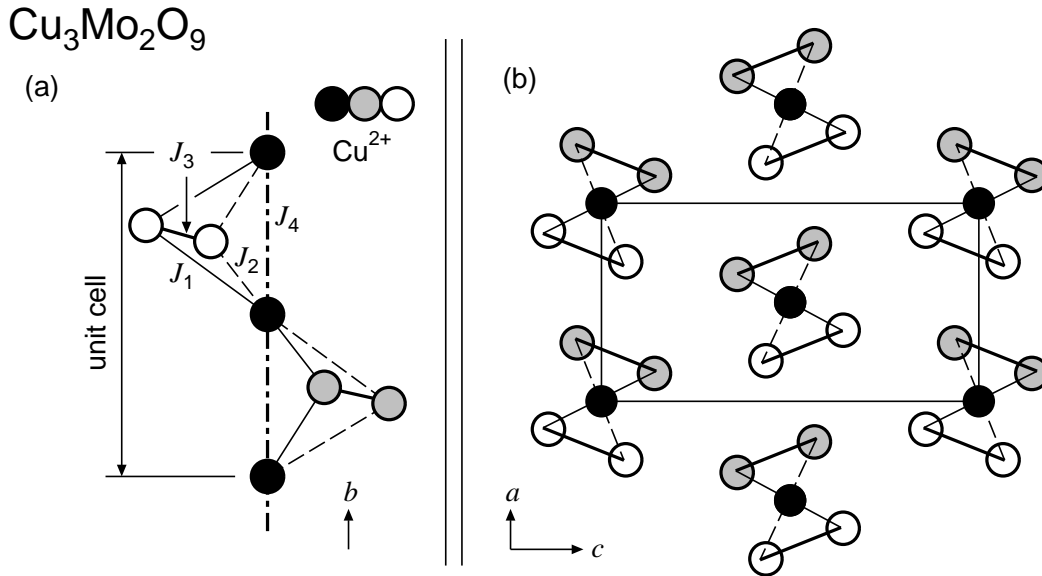


Fig. 1. Schematics of the distorted tetrahedral chain in $\text{Cu}_3\text{Mo}_2\text{O}_9$ along the b axis (a) and in the ac plane (b). The circles indicate the $S = 1/2$ Cu^{2+} ions and the symbols distinguish their coordinates along the b axis from others. O^{2-} and Mo^{4+} ions are omitted. The dashed, solid, bold and dot-dashed lines distinguish the superexchange interactions J_1 - J_4 between Cu^{2+} ions. The solid rectangle in (b) denotes the unit cell, which contains two tetrahedral chains.

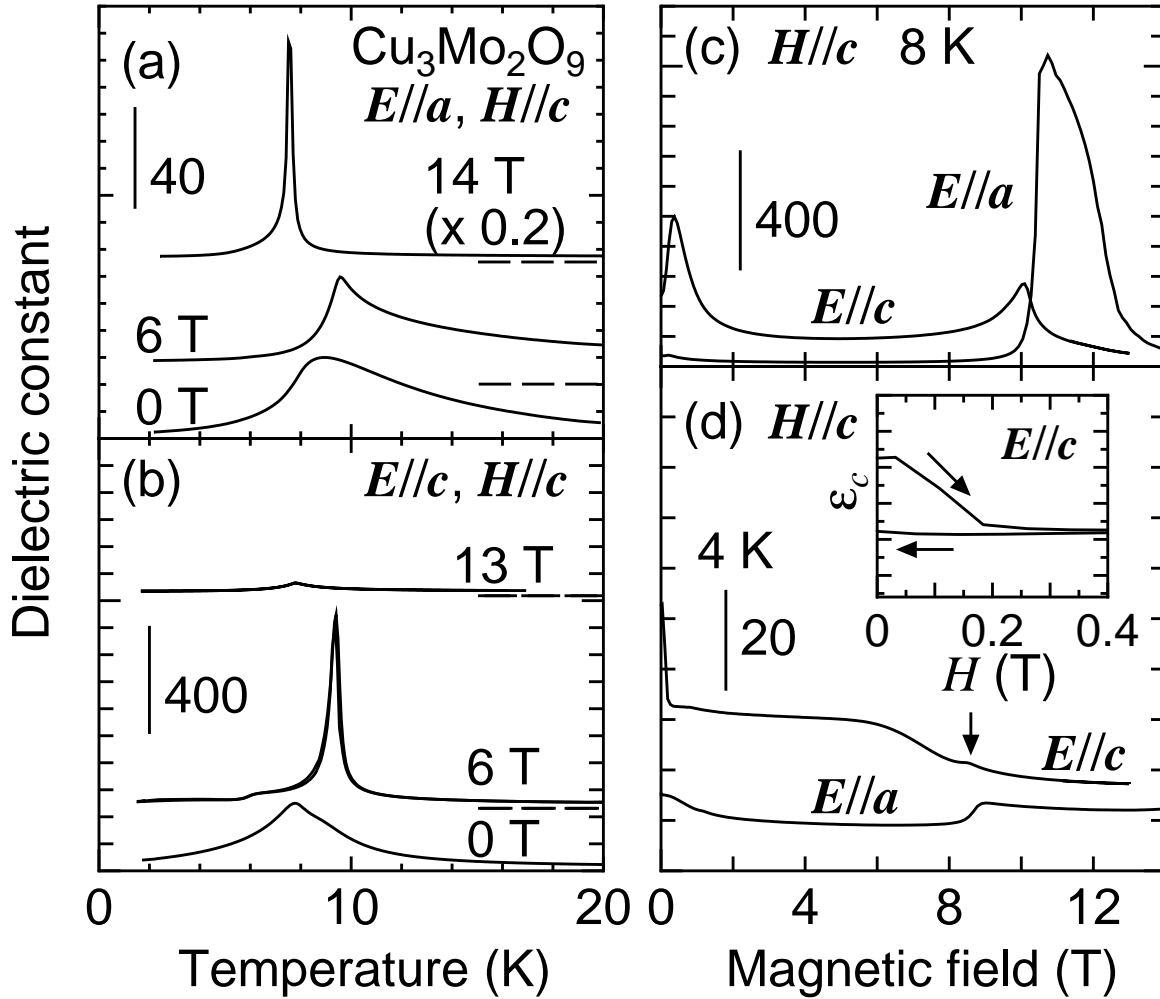


Fig. 2. Typical temperature dependences of the dielectric constants under fixed magnetic fields [(a) and (b)]. For the visibility, the data were shifted. The magnetic-field dependences of the dielectric constants at 8 and 4 K are shown in (c) and (d), respectively.

To form a capacitor, the faces were coated by gold and attached by two gold wires. The capacitance, of which the typical value was in the order of 10 pF, was measured by using the impedance analyzer (Yokogawa-Hewlett-Packard 4192A). ϵ_α was obtained from the capacitance at 100 kHz with a peak voltage of 1 V. To confirm the ferroelectric behavior, the electric polarization-electric field loop (the P_α - E_α loop) at 1 Hz was recorded by using a modified Sawyer-Tower circuit with a peak voltage of about 200 V. The magnetic field was applied by a superconducting magnet (Oxford Instruments, Teslatron S14/16), of which the maximum magnetic field was 16 T, and the variable temperature insert cryostat set temperature from 1.5 to 300 K.

Figures 2(a) and (b) show the typical T dependences of ϵ_α ($\alpha = a$ or c) under a fixed H (the ϵ_α - T curves), respectively, each of which has a (local) maximum value $\epsilon_\alpha^{\text{peak}}$ at T_α^{peak} . The

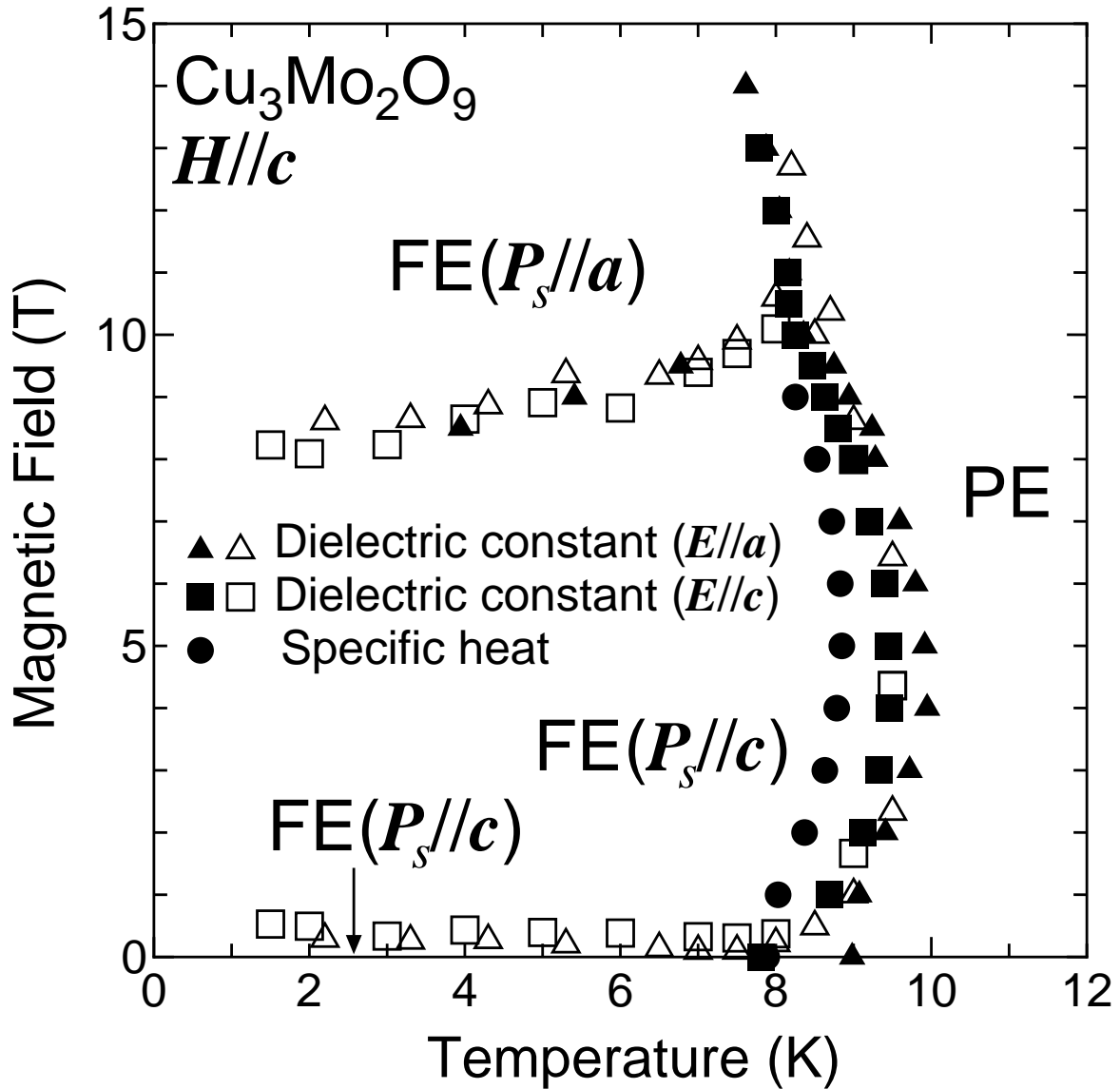


Fig. 3. The H - T phase diagram in $\text{Cu}_3\text{Mo}_2\text{O}_9$. The shape of symbols distinguish the physical quantities to be used to obtain the phase boundary. The triangles, squares and circles denote the dielectric constants along the a and c axes and specific heat, respectively. The solid (open) symbols denote the phase boundary obtained from the data of the $T(H)$ dependence.

values of T_α^{peak} against H are plotted in the H - T phase diagram by the solid symbols in Fig. 3. Figures 2(c) and (d) show the typical H dependences of ϵ_α at 8 and 4 K (the ϵ_α - H curves), respectively. At 8 K, as shown in Fig. 2(c), the ϵ_a - H and the ϵ_c - H curves have a peak and two ones, respectively. These are plotted in the phase diagram by the open symbols in Fig. 3. We observed a colossal magnetocapacitance (800%) at 8 K in Fig. 2(c). Here the maximum value of ϵ_a just above 10 T was compared with the minimum value of ϵ_a around 6 T. This magnetocapacitance is larger than the maximum one reported before.¹³⁾ Probably, this is due

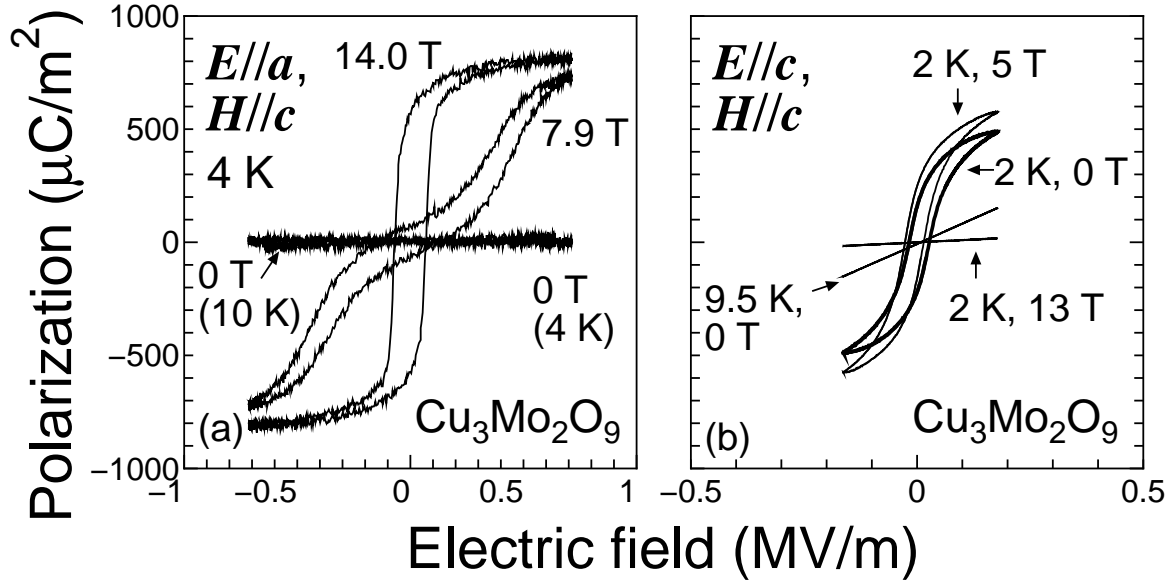


Fig. 4. Typical polarization-electric-field loops. Two loops at 4 and 10 K under 0 T in (a) almost overlap with each other.

to strong fluctuations around the tricritical point at $(H, T) = (10 \text{ T}, 8 \text{ K})$ in the H - T phase diagram. At 4 K, as shown in Fig. 2(d), ϵ_c gradually decreases with increasing H above 6 T. At about 8 T, a small peak is observed in the ϵ_c - H curve, which is indicated by an arrow and is plotted in Fig. 3 by an open symbol. Around this H , ϵ_a shows a sudden increase.

At 4 K, as shown in the inset of Fig. 2(d), the ϵ_c - H curve under the zero-magnetic-field cooling process rapidly decreases with increasing H from 0 T. This anomaly is not observed in the reducing magnetic field process. We plot H , where this hysteresis effect disappears, in Fig. 3. Around this H , the H dependence of the magnetization M_c (the M_c - H curve) along the c axis shows a small jump with a magnetic-field hysteresis effect.⁹⁾ In some multiferroic materials, the change of electric polarization accompanied by a jump of the magnetization has been reported.^{1,14)} These facts and the present result that the peaks in the ϵ_α - T curves become sharp at 6 T [Figs. 2(a) and (b)] suggest that the zero-field ground state contains some fluctuations, which is consistent with our picture describing the canted antiferromagnetism at zero and finite magnetic fields.^{9,15)} In this picture, the canting direction of the spin moment contains the randomness after zero-field cooling process. The jump of the magnetization in finite magnetic fields is understood as the alignment of the canting direction. Once it occurs, it survives even at zero magnetic field because of the internal magnetic field, indicating a possibility of the magnetic-field hysteresis effect in this system.

Together with the additional data and the phase boundary obtained from the T dependence of the specific heat under H ,¹⁰⁾ we obtain the H - T phase diagram in Fig. 3. One can see that the increase of T_α^{peak} at 6 T [Figs. 2(a) and (b)] corresponds to the change of T_N

under H .¹⁰⁾ We emphasize here that the peak in the ϵ_α - T (ϵ_α - H) curve is not necessarily in agreement with the critical temperature (magnetic field) of phase transition. And therefore, it is natural that the plots in the H - T phase diagram obtained from the data of ϵ_α do not trace perfectly the phase boundary obtained by using specific heat. We conclude that the phase diagram contains four different phases.

To observe the spontaneous electric polarization directly, we measured the P_α - E_α loop. Figures 4(a) and (b) show the typical results at various T and H . At 0 T, as shown in Fig. 4(b), the P_c - E_c loop below T_N shows a clear ferroelectric behavior. The value of the spontaneous electric polarization density ($\sim 500 \mu\text{C}/\text{m}^2$) is close to that in TbMnO_3 .¹⁾ As shown in Fig. 4(a), the P_a - E_a loop at 0 T does not show it. And then, we conclude that $\text{Cu}_3\text{Mo}_2\text{O}_9$ at 0 T below T_N is in the ferroelectric phase with a spontaneous electric polarization along the c axis [the $\text{FE}(\mathbf{P}_s//\mathbf{c})$ phase]. This result is consistent with the following facts: $\epsilon_c^{\text{peak}} \sim 10 \times \epsilon_a^{\text{peak}}$ in Figs. 2(a) and (b) and a strong microwave absorption was observed around T_N at zero magnetic field.

Figure 4(b) shows the H dependence of the P_c - E_c loop. At 5 T, the P_c - E_c loops indicates the $\text{FE}(\mathbf{P}_s//\mathbf{c})$ phase because it is almost similar to that at 0 T (The data was not shown). Instead of the closed P_c - E_c loop at 13 T, we observed the ferroelectric P_a - E_a loop at 14 T. The ϵ_a^{peak} at 13 T becomes about ten times larger than ϵ_a^{peak} at 6 T [Fig. 2(a)]. The ϵ_c^{peak} at 13 T becomes about ten times smaller than ϵ_c^{peak} at 6 T [Fig. 2(b)]. Judging from these results, we confirm the $\text{FE}(\mathbf{P}_s//\mathbf{a})$ phase at 13 T. The spontaneous electric polarization density ($\sim 800 \mu\text{C}/\text{m}^2$) is comparable to that in DyMnO_3 at 21 K.¹³⁾

As shown in Fig. 2(d) both the ϵ_a - H and ϵ_c - H curves show anomalies around 8 T at 4 K. As shown in Fig. 4(a), the P_a - E_a curve suggests a double hysteresis loop at 7.9 T. This effect is explained by the electric-field induced electric polarization and indicates strong fluctuations around the phase boundary. We conclude that the change of direction of the spontaneous electric polarization occurs at the phase boundary running from $(H, T) = (8 \text{ T}, 2 \text{ K})$ to $(10 \text{ T}, 8 \text{ K})$. Around 8 T, the change of electron-spin-resonance spectrum was reported.¹⁶⁾ Together with the phase transition temperatures obtained from the T dependences of M_c under various H ,¹⁰⁾ we conclude that this compound is a multiferroic material.

In many cases, the origin of the multiferroics has been discussed based on the formation of the magnetic superlattice. Unfortunately, the spin structure below T_N at 0 T has not been clarified yet. However, we emphasize again that the AFM long-range order below T_N has been established by the magnetic dispersion curve obtained from the inelastic-neutron scattering.¹²⁾ Moreover, the anisotropic magnetization has been quantitatively explained based on a weakly canted AFM long-range order.⁹⁾

The point of discussion is how the AFM long-range order induces ferroelectricity. In the following, we focus on the charge redistribution effects caused by the three-spin ring exchange

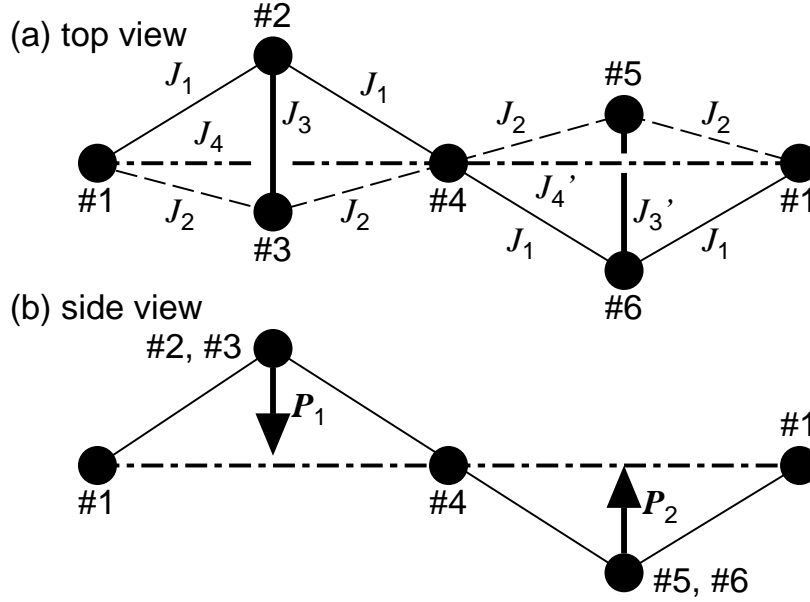


Fig. 5. Six-spin cluster under the periodic-boundary condition. $\#i$ indicates the i -th $S=1/2$ spin. This spin cluster can be divided into two tetrahedral spin clusters, each of which has an electric polarization \mathbf{P}_1 or \mathbf{P}_2 . The charge redistribution at the center site ($\#4$) is divided so that both the \mathbf{P}_1 and \mathbf{P}_2 exist on the bisector between the sites $\#1$ and $\#4$.

interaction in geometrically frustrated Mott insulators, proposed by Bulaeviskii *et al.*^{7,8)} We demonstrate that the spin cluster in Fig. 5 has a potential of the multiferroic behavior as a result of the *antiferroelectric* (AFE) polarization at zero electric field and the *ferrielectric* (FRE) polarization under an electric field. This is the minimum system which keeps the tetrahedral spin arrangement and the inversion center at the spin site $\#4$ simultaneously and the formation of the magnetic superlattice is impossible.

We treat this system as a Mott insulator. The electronic band from the $d_{x^2-y^2}$ orbitals in the Cu^{2+} ions is half-filled. In the limit of the strong on-site Coulomb repulsion U , where the charge degrees of freedom are frozen, the system can be mapped on the quantum spin system. The spin Hamiltonian is given by

$$\mathcal{H} = \sum_{\langle i,j \rangle} \frac{4t_{ij}^2}{U} \mathbf{S}_i \cdot \mathbf{S}_j + \sum_i g\mu_B \mathbf{S}_i \cdot \mathbf{H}_i^{\text{loc}}, \quad (1)$$

where the sum in the first term of the right-hand side runs over all the possible spin pairs (\mathbf{S}_i and \mathbf{S}_j at the $\#i$ and $\#j$ sites, respectively) connected through the hopping parameter t_{ij} . The values of $4t_{ij}^2/U$ correspond to the exchange interactions in Fig. 5. The second term in the right-hand side is the magnetic energy from the local magnetic field $\mathbf{H}_i^{\text{loc}}$ at the $\#i$ site, where g and μ_B are the g factor and the Bohr magneton, respectively.

Based on the interchain interaction in $\text{Cu}_3\text{Mo}_2\text{O}_9$,¹²⁾ we set the values $J_1 = J_2 = 1$ meV,

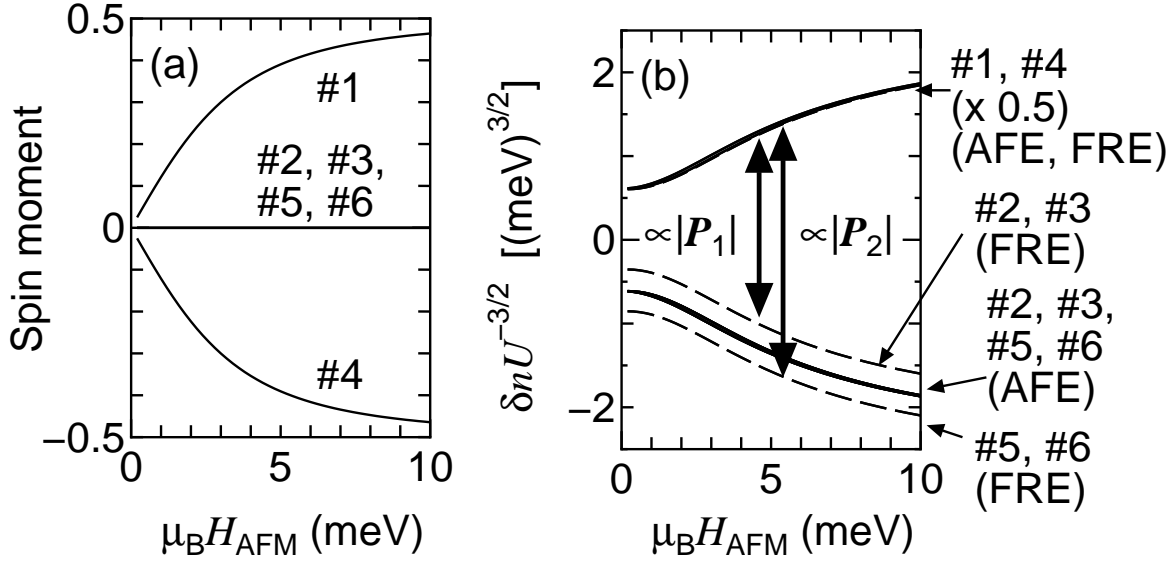


Fig. 6. The spin moments projected on the quantum axis (a) and the charge redistributions (b) in the six-spin cluster under the periodic-boundary condition as functions of the staggered magnetic field. The parameter sets which give the antiferroelectric (AFE) and ferroelectric (FRE) phases are given in the text. The electric polarizations are shown by the arrows.

$J_3 = J'_3 = 5.8$ meV, $J_4 = 4$ meV and $g = 2$. We introduced the staggered magnetic field $H_{\text{AFM}} \equiv |\mathbf{H}_i^{\text{loc}}|$ along the quantization axis working on only the #1 and #4 sites. H_{AFM} induces the AFM spin order at the site on the spatial inversion symmetry, i.e., this site is on the anti-inversion center in the word of the magnetic space group. By using the exact-diagonalization, we calculated $\langle \mathbf{S}_i \rangle$ and the charge redistribution δn_i at the spin site # i :^{7,8)}

$$\delta n_i = \sum_{\langle i,j,k \rangle} \frac{8t_{ij}t_{jk}t_{ki}}{U^3} [\mathbf{S}_i \cdot (\mathbf{S}_j + \mathbf{S}_k) - 2\mathbf{S}_j \cdot \mathbf{S}_k] , \quad (2)$$

in the periodic-boundary six-spin cluster at 0 K. Here the sum in the right-hand side runs over all the possible spin triangle connected by the exchange interactions. The amplitude of an electric polarization $|\mathbf{P}_{1(2)}|$ is proportional to $\delta n_{1(5)} - \delta n_{2(1)} - \delta n_{3(4)} + \delta n_{4(6)}$,

As shown in Figs. 6(a) and (b), $|\langle \mathbf{S}_{\{1,4\}} \rangle_z|$ and $|\mathbf{P}_{\{1,2\}}|$ become large with increasing H_{AFM} . Even in this case, the spins at the sites #2, #3, #5 and #6 still form the nonmagnetic spin dimers. We plot $\delta n U^{-3/2}$ in Fig. 6(b) because we could not estimate a precise value of U , and the calculations in the larger system are necessary to discuss the origin of the finite $|\mathbf{P}_{\{1,2\}}|$ without the staggered magnetic field because of the strong system-size dependences.

Under a uniform electric field, the exchange interaction is slightly changed as a result of the breaking of the spatial inversion symmetry.¹⁷⁾ If the exchange interactions of the nonmagnetic spin dimers are different ($J_3 = 5.0$ meV and $J'_3 = 6.6$ meV), we obtain the finite net electric dipole moment as a result of the FRE alignment of the electric dipoles ($\mathbf{P}_1 \neq -\mathbf{P}_2$) even

though the $\langle \mathbf{S}_i \rangle$ is not changed. From this calculation, we conclude that the tetrahedral quasi-one dimensional spin system has a potential of the AFM-AFE and AFM-FRE type multiferroic behaviors. The finite net electric dipole moment appears when the time and spatial inversion symmetries are broken.

In this letter, we demonstrate a possibility of electric polarization induced by the antiferromagnetic long-range order in the distorted tetrahedral quasi-one dimensional spin system. As an experimental evidence, we showed the H - T phase diagram of $\text{Cu}_3\text{Mo}_2\text{O}_9$ under the magnetic field along the c axis by studying the temperature and a magnetic-field dependences of the dielectric constant. The ferroelectric behavior was observed in the polarization-electric-field loop and the change of the polarization direction was found. Around the tricritical point at (10 T, 8 K), a colossal magnetocapacitance was observed. We showed that the six-spin cluster which corresponds to the tetragonal quasi-one dimensional spin system has a potential to undergo the AFM-AFE multiferroic state without a formation of the magnetic superlattice. The possibility of the AFM-FRE multiferroic state under the electric field was discussed.

Acknowledgments

This work is partly supported by a Grant-in-Aid for Scientific Research (C) (No. 40296885) and that on Priority Area (No. 19052005) from the Ministry of Education, Culture, Sports, Science and Technology of Japan (MEXT). We acknowledge Dr. N. Terada in NIMS, Dr. Y. Nishiwaki and Prof. T. Nakamura in Shibaura Institute of Technology, Prof. T. Goto, Dr. M. Akaki and Prof. H. Kuwahara in Sophia University for helpful discussions. We also wish to acknowledge the technical assistance of Mr. R. Kino and Mr. M. Suzuki.

References

- 1) T. Kimura, T. Goto, H. Shintani, K. Ishizawa, T. Arima and Y. Tokura: Nature **426** (2003) 55.
- 2) For review, S-W Cheong and M. Mostovoy: Nature Mat. **6** (2007) 13.
- 3) H. Katsura, N. Nagaosa and A. V. Balatsky: Phys. Rev. Lett. **95** (2005) 057205.
- 4) M. Kenzelmann, A. B. Harris, S. Jonas, C. Broholm, J. Schefer, S. B. Kim, C. L. Zhang, S.-W. Cheong, O. P. Vajk and J. W. Lynn: Phys. Rev. Lett. **95** (2005) 087206.
- 5) M. Mostovoy: Phys. Rev. Lett. **96** (2006) 067601.
- 6) T. Arima, T. Goto, Y. Yamasaki, S. Miyasaka, K. Ishii, M. Tsubota, T. Inami, Y. Murakami and Y. Tokura: Phys. Rev. B **72** (2005) 100102R.
- 7) L. N. Bulaevskii, C. D. Batista, M. V. Mostovoy and D. I. Khomskii: Phys. Rev. B **78** (2008) 024402.
- 8) D. I. Khomskii: J. Phys.: Condens. Matter **22** (2010) 164209.
- 9) T. Hamasaki, N. Ide, H. Kuroe, T. Sekine, M. Hase, I. Tsukada and T. Sakakibara: Phys. Rev. B **77** (2008) 134419.
- 10) T. Hamasaki, H. Kuroe, T. Sekine, M. Akaki, H. Kuwahara and M. Hase: J. Phys.: Conf. Ser. **200** (2010) 022013.
- 11) H. Kuroe, T. Hamasaki, T. Sekine, M. Hase, K. Oka, T. Ito, H. Eisaki and M. Matsuda: J. Phys.: Conf. Ser. **200** (2010) 022028.
- 12) H. Kuroe, T. Hamasaki, T. Sekine, M. Hase, K. Oka, T. Ito, H. Eisaki, K. Kaneko, N. Metoki, M. Matsuda and K. Kakurai: Phys. Rev. B **83** (2011) 184423.
- 13) T. Goto, T. Kimura, G. Lawes, A. P. Ramirez and Y. Tokura: Phys. Rev. Lett. **92** (2004) 257201.
- 14) T. Kimura, J. C. Lashley and A. P. Ramirez: Phys. Rev. B **73** (2006) 220401R.
- 15) M. Hase, H. Kitazawa, K. Ozawa, T. Hamasaki, H. Kuroe and T. Sekine: J. Phys. Soc. Jpn. **77** (2008) 034706.
- 16) S. Okubo, T. Yoshida, M. Fujisawa, T. Sakurai, H. Ota, T. Hamasaki, H. Kuroe, T. Sekine, M. Hase, K. Oka, T. Ito and H. Eisaki: J. Low Temp. Phys. **159** (2010) 32.
- 17) M. Trif, F. Troiani, D. Stepanenko and D. Loss: Phys. Rev. B **82** (2010) 045429.